JOC Article

Dynamic Helical Chirality of an Intramolecularly Hydrogen-Bonded Bisoxazoline†

Adam J. Preston, Gideon Fraenkel, Albert Chow, Judith C. Gallucci, and Jon R. Parquette*

Department of Chemistry, The Ohio State University, Columbus, Ohio 43210

parquett@chemistry.ohio-state.edu

Received September 30, 2002

The synthesis and conformational properties of 2,6-bis-[2-((4*S*)-4-methyl-4,5-dihydro-1,3-oxazol-2-yl)phenyl]carbam oylpyridines, **2**, have been described. Bisoxazoline **2a** was prepared in five steps from 2-nitrobenzoyl chloride in an overall yield of 71%. In contrast to related structures such as **1**, bisoxazoline **2a** exhibits a highly biased P-type helical conformation in solution and in the solid state. In the crystal lattice, **2a** further assembles into a left-handed helical superstructure aligned along the crystallographic *c* axis. The barrier to helical interconversion, as measured by line-shape analysis of the temperature-dependent ^{1}H NMR spectra of thiobenzyl derivative **2b**, was determined to be quite low ($\Delta G^{\ddagger} = 12.3$ kcal/mol), indicating the presence of a highly dynamic helical chirality.

Introduction

The helix represents an important example of conformational chirality that is ubiquitous in the structure of biomolecules[1] and extensively exploited in asymmetric catalysis.[2] Conformational chirality has been observed primarily in compounds displaying atropisomerism such as helicenes,[3] substituted biphenyls,[4] 1,1′-bi-2-binaphyls,[5] molecular propellers,[6] "geländer" molecules,[7] transition-metal complexes,[8] and cyclophanes.[9] Occasionally, compounds having chiral conformations with low barriers to racemization spontaneously resolve during crystallization into a single conformational enantiomer but racemize in solution.[10] Although the use of highly rigid, preorganized structures in functional materials and supramolecular chemistry has been a successful design strategy, it has recently been suggested that overly constrained synthetic catalysts and receptors are less effective, because in these rigid systems binding affinity and specificity are interdependent.[11] Therefore, molecules exhibiting helical chirality based on the presence of a dynamic and highly biased conformational equilibrium have potential to serve as molecular scaffolds upon which to build structural adaptability into functional materials.

Pyridine-2,6-dicarboxamides exist primarily in the syn,syn conformation, because this conformation places the amide NH groups in close proximity to the pyridine-*N*, which permits intramolecular hydrogen-bonding interactions to occur. Further, this orientation of the amides minimizes the repulsive electrostatic interactions between the amide oxygens.[12] This conformational preference has been exploited as a scaffold to create helical structures, because groups linked through the carboxamides are constrained in a manner that positions them above and below the plane of the pyridine moiety, resulting in a local helical structure.[13] However, interconversion between the helical antipodes is fast relative to the NMR time scale, and chiral derivatives have not exhibited a significant helical diastereomic bias in solution.[14]

Structure **1** folds into a helical conformation due to hydrogen-bonding of the amide N−H's with the pyr-N and carbonyl oxygens (Chart 1). In solution, we observed

† Dedicated to the honor and memory of Prof. Henry Rapoport.

(1) Creighton, T. E. *Proteins: Structures and Molecular Properties*, 2nd ed.; W. H. Freeman: New York, 1993.

(2) For a review, see: Ojima, I. *Catalytic Asymmetric Synthesis*; VCH: Weinheim, 2000.

(3) (a) Dreher, S. D.; Weix, D. J.; Katz, T. J. *J. Org. Chem.* **1999**, *64*, 3671. (b) Furche, F.; Ahlrichs, R.; Wachsmann, C.; Weber, E.; Sobanski, A.; Voegtle, F.; Grimme, S. *J. Am. Chem. Soc.* **2000**, *122*, 1717.

(4) (a) Theilacker, W.; Hopp, R. *Chem. Ber.* **1959**, *92*, 2293. (b) Theilacker, W.; Boehn, H. *Angew. Chem., Int. Ed. Engl.* **1967**, *6*, 251.

(5) (a) Noyori, R.; Takaya, H. *Acc. Chem. Res.* **1990**, *23*, 345. (b) Noyori, R. *Stereocontrolled Org. Synth.* **1994**, 1.

(6) Rappoport, Z.; Biali, S. E. *Acc. Chem. Res.* **1997**, *30*, 307.

(7) Kiupel, B.; Niederalt, C.; Nieger, M.; Grimme, S.; Vogtle, F. *Angew. Chem., Int. Ed. Engl.* **1998**, *37*, 3031.

(8) Djukic, J.-P.; Michon, C.; Maisse-Francois, A.; Allagapen, R.; Pfeffer, M.; Dotz, K. H.; De Cian, A.; Fischer, J. *Chem. Eur. J.* **2000**, *6*, 1064 and references therein.

(9) Grimme, S.; Harren, J.; Sobanski, A.; Voegtle, F. *Eur. J. Org. Chem.* **1998**, 1491.

(10) (a) Azumaya, I.; Okamoto, I.; Nakayama, S.; Tanatani, A.; Yamaguchi, K.; Shudo, K.; Kagechika, H. *Tetrahedron* **1999**, *55*, 11237. (b) Cunningham, I. D.; Coles, S. J.; Hursthouse, M. B. *Chem. Commun.* **2000**, 61.

(11) (a) Davis, A. M.; Teague, S. J. *Angew. Chem., Int. Ed. Engl.* **1999**, *38*, 736. (b) Sanders, J. K. M. *Chem. Eur. J.* **1998**, *4*, 1378. (c) Szwajkajzer, D.; Carey, J. *Biopolymers* **1997**, *44*, 181.

(12) For a computational study, see: Malone, J. F.; Murray, C. M.; Dolan, G. M.; Docherty, R.; Lavery, A. J. *Chem. Mater.* **1997**, *9*, 2983.

(13) (a) Hamuro, Y.; Geib, S. J.; Hamilton, A. D. *J. Am. Chem. Soc.* **1997**, *119*, 10587. (b) Hamuro. Y.; Geib, S. J.; Hamilton, A. D. *J. Am. Chem. Soc.* **1996**, *118*, 7529. (c) Crisp, G. T.; Jiang, Y.-L. *Tetrahedron* **1999**, *55*, 549.

(14) (a) Kawamoto, T.; Prakash, O.; Ostrander, R.; Rheingold, A. L.; Borovik, A. S. *Inorg. Chem.* **1995**, *34*, 4294. (b) Yu, Q.; Baroni, T. E.; Liable-Sands, L.; Rheingold, A. L.; Borovik, A. S. *Tetrahedron Lett.* **1998**, *39*, 6831. (c) Baroni, T. E.; Liable-Sands, L.; Rheingold, A. L.; Borovik, A. S. *Tetrahedron Lett.* **1998**, *39*, 6831. (d) Kawamoto, T.; Hammes, B. S.; Ostrander, R.; Rheingold, A. L.; Borovik, A. S. *Inorg. Chem.* **1998**, *37*, 3424. (e) Crisp, G. T.; Jiang, Y.-L. *Tetrahedron* **1999**, *55*, 549. (f) Moriuchi, T.; Nishiyama, M.; Yoshida, K.; Ishikawa, T.; Hirao, T. *Org. Lett.* **2001**, *3*, 1459. (g) Shirin, Z.; Thompson, J.; Liable-Sands, L.; Yap, G. P. A.; Rheingold, A. L.; Borovik, A. S. *J. Chem. Soc., Dalton. Trans.* **2002**, 1714.

10.1021/jo026496f CCC: $25.00
Published on Web 12/04/2002

CHART 1

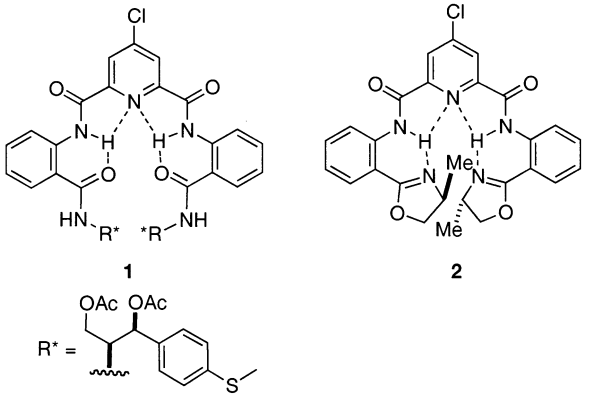

a chiral helical bias only when this structure was incorporated as a peripheral unit in dendrimers rigidified through hydrogen bonding.[15] The conformational chirality that occurs in dendrimers, but not in the monomer **1**, was attributed to the correlated molecular motion that occurs at the periphery of the dendrimers, which increased the energetic difference between the helical antipodes. The goal of the current research was directed at developing low molecular weight molecules displaying dynamically biased, helical conformations, which also may potentially serve as ligands for transition metals. We reasoned that rigidifying the helical conformation by replacing the amide carbonyls, which interact with the N−H's via a relatively weak ═O···H−N H-bond, with oxazoline moieties capable of stronger ═N···H−N H-bonding interactions, as shown in structure **2**, would lead to greater helical bias. Furthermore, molecular modeling studies suggested that in the lowest energy conformation, the methyl substituents of the oxazoline groups interact more strongly in the M than in the P helical conformation.[16]

Results and Discussion

Synthesis. Bisoxazoline **2a** was prepared in five steps with an overall yield of 71% from 2-nitrobenzoyl chloride (Scheme 1). Synthesis proceeded by amidation of 2-nitrobenzoyl chloride with L-alaninol followed by chlorination of the resultant alcohol, **4a**, with thionyl chloride affording chloride **4b**. Ring closure with sodium hydride to oxazoline **5a**, reduction of the nitro function by hydrogenation over Pd−C, and final reaction with 4-chloropyridine-2,6-dicarbonyl dichloride afforded **2a**. The ^{1}H NMR spectrum of **2a** in $CDCl_3$ was consistent with the presence of stronger hydrogen-bonding interactions between the N−H's and the ═N of the oxazolines relative to the ═O of the carbonyls in **1**. Whereas for **1** a single resonance was observed for the N−H's at 12.7 ppm,[17] **2a** exhibited a low-field resonance for the N−H's at 13.7 ppm.

Solution Structure. Helical Interconversion Barrier. The fluxional nature of the molecule was evident in the ^{1}H NMR spectrum of **2b** in THF-d_8 (Figure 1). At low temperature, the methylene hydrogens of the thiobenzyl group appear as a well-defined AB quartet due to the global helical conformation of the molecule. Interestingly, at temperatures where the rate of helical interconversion was slow on the NMR time scale, only a single helical diastereomer was evident, indicating an extremely biased conformational equilibrium. Increasing temperature caused the AB quartet to gradually coalesce into a singlet, consistent with the progressive averaging of the two protons undergoing A−B exchange due to an M⇔P helical interconversion. However, both the A and B proton chemical shifts as well as the difference between them ($\delta_A - \delta_B$) varied with temperature. Therefore, to calculate the rate constants for interconversion it was necessary to estimate the intrinsic $\delta_A - \delta_B$ at a temperature where signal averaging was observed.[18] This was done by plotting the observed $\delta_A - \delta_B$ values over the temperature range in which an AB spectrum could be discerned (−90 → −20 °C) and then extrapolating to a temperature at which A−B averaging takes place (−10 °C). A−B line shapes were then calculated as a function of k_1, the rate constant for helical interconversion, using the extrapolated $\delta_A - \delta_B$ value and the observed J_{A-B} coupling constant (12.76 Hz).[18] Matching the experimental and calculated NMR spectra provided the first-order rate constant for helical interconversion ($k_1 = 345\ s^{-1}$). This rate constant corresponds to a $\Delta G^{\ddagger}$ value of 12.3 kcal for the barrier to helical interconversion. Therefore, the helical diastereomers rapidly interconvert at ambient temperature.

Circular Dichroism. Absolute Stereochemistry of Helical Structure. The stereochemistry of the helical bias in solution was determined by circular dichroism (CD) spectroscopy (Figure 2). The ultraviolet (UV) spectrum of **2a** in acetonitrile displayed absorptions at 216, 253, and 309 nm. Accordingly, the CD spectrum of **2a** in acetonitrile showed a positive Cotton effect (CE) at 216 nm, a negative CE at 253 nm, and a bisignet couplet having a negative CE at 300 nm, a positive CE at 328, and a zero-crossing at 309 nm. The peaks at 216 and 253 nm are simple CEs associated with the corresponding transitions in the UV spectra at 216 and 256 nm, respectively. The bisignet couplet centered at 309 nm shows excitonic splitting with positive chirality, as defined by Nakanishi and Harada.[19]

N-[2-(4-Methyl-4,5-dihydrooxazol-2-yl)phenyl]acetamide (**6**) also exhibited a transition in the UV spectrum at 309 nm, indicating that this chromophore was responsible for the transition at 309 nm for **2a**. Time-dependent density-functional (TDDFT) methods[20] were applied to **6**, using the three-parameter Lee−Yang−Parr (B3LYP) functional[21] and the 6−31g* basis set, to model the 2-acylaminophenyl oxazoline moieties of **2a** responsible for the transition at 309 nm (Figure 3). Prior to performing the TDDFT electronic structure calculations, the geometry of **6** was optimized using the B3LYP functional also employing the 6−31g* basis set.[22] The lowest energy transition corresponded to a $\pi \rightarrow \pi^*$ transition at 296 nm, in reasonable agreement with the experimental value of

(15) (a) Recker, J.; Tomcik, D. J.; Parquette, J. R. *J. Am. Chem. Soc.* **2000**, *122*, 10298.(b) Huang, B.; Parquette, J. R. *J. Am. Chem. Soc.* **2001**, *123*, 2689.

(16) A Monte Carlo conformational search using the MM2* force field as implemented in Macromodel 6.0 predicted that the P helical conformation was favored over the M helix by 0.8 kcal/mol.

(17) Huang, B.; Parquette, J. R. *Org. Lett.* **2000**, *2*, 239.

(18) Kaplan, J. I.; Fraenkel, G. *NMR of Chemically Exchanging Systems*; Academic Press: New York, 1960; pp 101−104.

(19) Harada, N.; Nakanishi, K. O. *Circular Dichroic Spectroscopy: Exciton Coupling in Organic Stereochemistry*; University Science Books: Mill Valley, CA, 1983.

SCHEME 1[a]

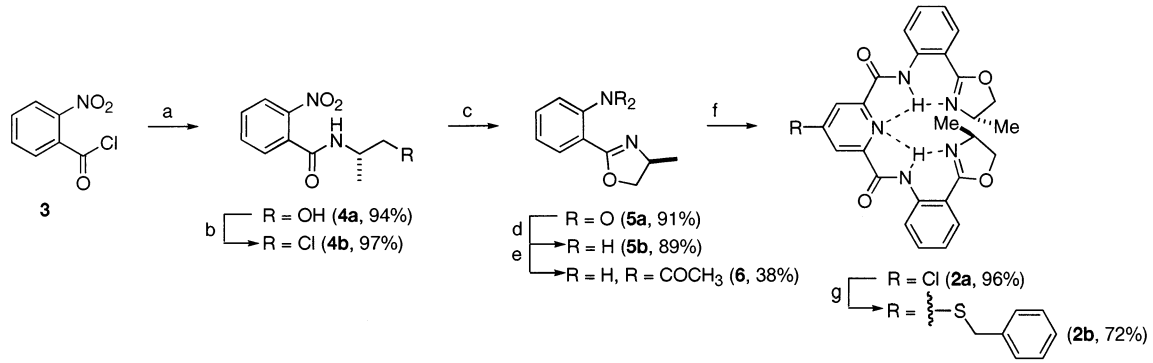

[a] Reagents: (a) (*S*)-2-amino-1-propanol, CH_2Cl_2, $(C_2H_5)_3N$. (b) $SOCl_2$, $CHCl_3$, reflux. (c) NaH, THF. (d) H_2/Pd−C, EtOAc. (e) Ac_2O, CH_2Cl_2, $(C_2H_5)_3N$, DMAP (cat.). (f) 4-Chloropyridine-2,6-dicarbonyl dichloride, Pyr-CH_2Cl_2. (g) $PhCH_2SH$, NaH, THF.

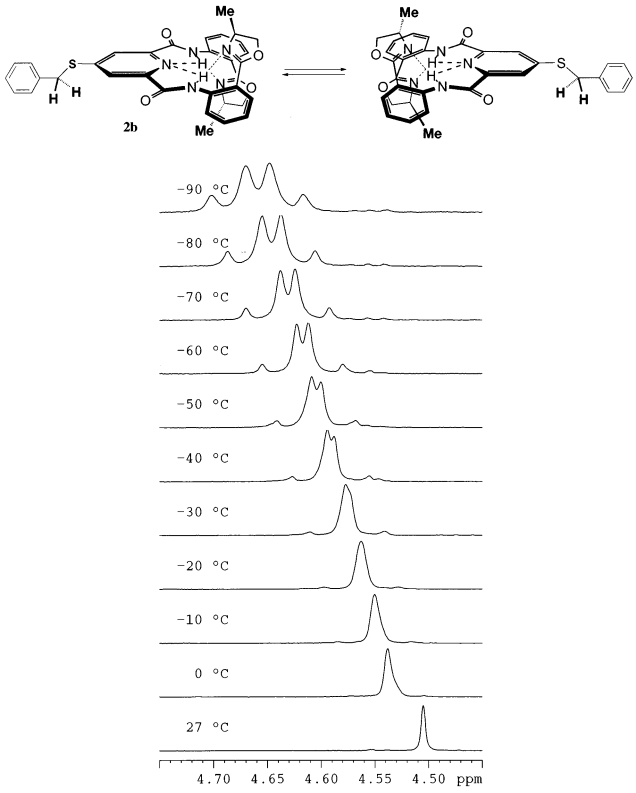

FIGURE 1. Temperature-dependent ^{1}H NMR spectra of **2b** in THF-d_8.

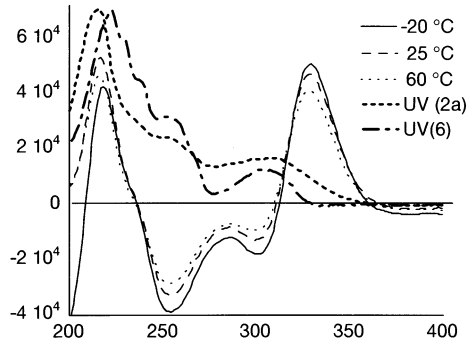

FIGURE 2. UV (arbitrary scale) and molar CD spectra of **2a** in acetonitrile.

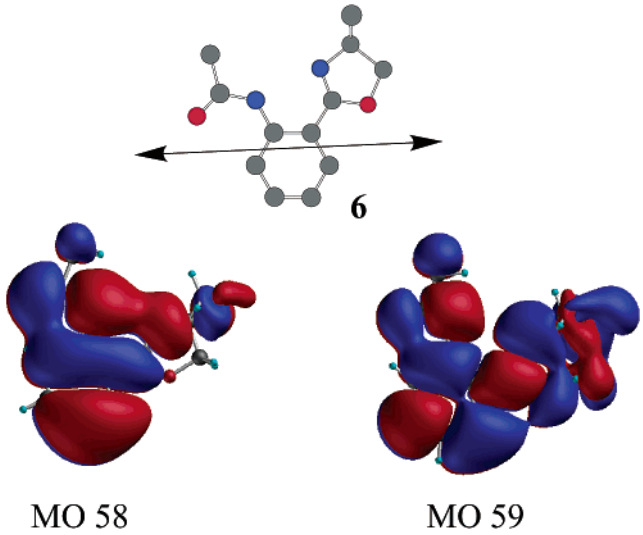

FIGURE 3. Molecular orbitals and electric transition dipole moment of the $\pi \rightarrow \pi^*$ transition at 309 nm, calculated by TDDFT using the 6−31g* basis set.

this electronic absorption. Inspection of the excitations that contribute to the transition at 296 nm indicates that the transition is dominated by an excitation that promotes an electron from a π molecular orbital (MO 58) to a π^* orbital (MO 59). The electric transition dipole moment runs approximately along the axis containing C-3 and C-6 of **6**, as shown in Figure 3. Therefore, the

(20) The TDDFT-B3LYP calculations were run as implemented in M. J. Frisch, G. W. Trucks, H. B. Schlegel, G. E. Scuseria, M. A. Robb, J. R. Cheeseman, V. G. Zakrzewski, J. A. Montgomery, Jr., R. E. Stratmann, J. C. Burant, S. Dapprich, J. M. Millam, A. D. Daniels, K. N. Kudin, M. C. Strain, O. Farkas, J. Tomasi, V. Barone, M. Cossi, R. Cammi, B. Mennucci, C. Pomelli, C. Adamo, S. Clifford, J. Ochterski, G. A. Petersson, P. Y. Ayala, Q. Cui, K. Morokuma, D. K. Malick, A. D. Rabuck, K. Raghavachari, J. B. Foresman, J. Cioslowski, J. V. Ortiz, A. G. Baboul, B. B. Stefanov, G. Liu, A. Liashenko, P. Piskorz, I. Komaromi, R. Gomperts, R. L. Martin, D. J. Fox, T. Keith, M. A. Al-Laham, C. Y. Peng, A. Nanayakkara, M. Challacombe, P. M. W. Gill, B. Johnson, W. Chen, M. W. Wong, J. L. Andres, C. Gonzalez, M. Head-Gordon, E. S. Replogle, and J. A. Pople, *Gaussian 98*, Revision A.7.; Gaussian, Inc.: Pittsburgh, PA, 1998.

(21) (a) Bauernschmitt, R.; Ahlrichs, R. *Chem. Phys. Lett.* **1996**, *256*, 454. (b) Stratmann, R. E.; Scuseria, G. E.; Frisch, M. J. *J. Chem. Phys.* **1998**, *109*, 8218. (c) Foresman, J. B.; Head-Gordon, M.; Pople, J. A.; Frisch, M. J. *J. Phys. Chem.* **1992**, *96*, 135.

(22) Hehre, W. J.; Radom, L.; Schleyer, P. V. R.; Pople, J. A. *Ab initio Molecular Orbital Theory*; John Wiley & Sons: New York, 1986.

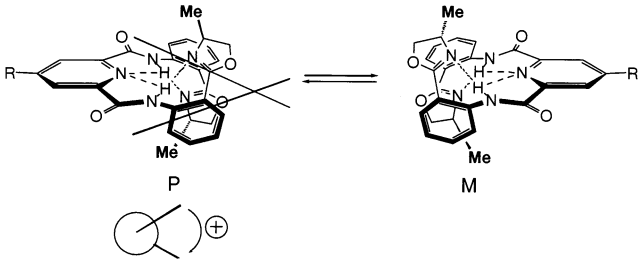

FIGURE 4. Interconversion between M and P helical conformations: the relative orientation of electric transition moments (positive chirality) indicates P helical conformational bias.

absolute sense of helical chirality relating the 2-acylaminophenyl oxazoline chromophores in solution can be assigned to be P, as shown in Figure 4 using the exciton chirality method pneumonic. The insensitivity of the couplet to temperature indicates that a highly biased helical secondary structure is present in **2a**.

Solid-State Conformation. A clear, tetragonal crystal in space group $P4_1$ was obtained for **2a** by crystallization from CH_2Cl_2/EtOAc.[23] X-ray diffraction showed that the asymmetric unit was composed of two virtually identical molecules exhibiting P helical chirality, in agreement with the CD studies (Figure 5). This helical conformation is induced by four hydrogen-bonding interactions between the pyridyl amide NH's and both the pyridine-N, with an average N−N distance of 2.685 Å, and the oxazoline-N's with an average N−N distance of 2.704 Å. These hydrogen-bonding interactions force the oxazoline rings to be placed in a face-to-face stacked arrangement that projects the methyl substituents above and below the plane of the helix, resulting in a P helical chirality. In the crystal lattice, **2a** further assembles into a left-handed helix aligned along the crystallographic *c* axis.[24] The helical superstructure is primarily stabilized by edge-to-face stacking interactions between the 2-acylaminophenyl rings of adjacent asymmetric units, with an average $C_{edge}-C_{face}$ distance of 3.74 Å. Presumably for electrostatic reasons, the two molecules of the asymmetric unit are packed in an arrangement orienting the C−Cl bond of one molecule antiparallel to a pyridyl amide C═O bond of the other molecule having (Cl)C···O(═C) and (C)Cl···C(═O) distances of 3.463 and 3.622 Å, respectively.

Conclusion

We conclude that the increased structural rigidity imparted to bisoxazoline **2** by the stronger intramolecular ═N···H−N H-bonding interactions, relative to **1**, causes a highly biased helical equilibrium to develop at low molecular weights. Although the low barrier to helical interconversion produces a highly dynamic conformational equilibrium at ambient temperature, a strong bias for the P helical sense is present in solution and in the solid state. We are currently investigating the conformational and catalytic properties of associated metal complexes of **2**.

(23) Crystallographic information: $T = 150(2)$ K; $P4_1$, $a = 8.951(1)$ Å, $c = 61.611(1)$ Å.; V = 4935.9(8) Å^3; $Z = 8$; 8656 unique data; R1(F) = 0.029, wR2(F^2) = 0.053; GOF = 1.044.

(24) For related, solid-state helical superstructures, see ref 14a,f.

Experimental Section

General. Melting points were determined in open capillaries and are uncorrected. ^{1}H NMR spectra were recorded at 400 MHz and ^{13}C NMR spectra at 100 MHz. Electrospray mass spectra were recorded at The Ohio State University Chemical Instrument Center. Circular dichroism (CD) measurements were carried out using optical grade solvents and quartz glass cuvettes with a 10 mm path length. All reactions were performed under an argon or nitrogen atmosphere. Dimethylformamide (DMF) was dried by distillation from activated 4 Å sieves; THF was distilled from sodium/benzophenone ketyl; pyridine, triethylamine, and dichloromethane were distilled from calcium hydride; and $CHCl_3$ was distilled from $CaCl_2$. Chromatographic separations were performed on silica gel 60 (230−400 mesh, 60 Å) using the indicated solvents.

***N*-(2-Hydroxy-(1*S*)-1-methylethyl)-2-nitrobenzamide (4a).** 2-Nitrobenzoyl chloride was prepared by adding oxalyl chloride (1.27 g, 0.87 mL, 10.0 mmol) to a solution of 2-nitrobenzoic acid (0.84 g, 5.00 mmol) and DMF (2 drops) in CH_2Cl_2 (10 mL). After stirring for 2 h, the solution became homogeneous and was concentrated in vacuo. The residue was dissolved in CH_2Cl_2 (2 × 5 mL) and added over the course of 1 h to a solution of *S*-(+)-2-amino-1-propanol (0.45 g, 467 μL, 6.00 mmol), Et_3N (1.5 g, 2.1 mL, 15.0 mmol), and 4 Å molecular sieves (ca 0.5 g) in CH_2Cl_2 (20 mL) at 0 °C. The reaction was allowed to warm to ambient temperature over 2 h. The molecular sieves were removed by filtration, and the solution was concentrated. The resultant residue was purified by column chromatography on silica using 50% CH_2Cl_2/EtOAc. Product was isolated as a white crystalline solid (1.06 g, 4.73 mmol, 94%): mp 90−91 °C (CH_2Cl_2); ^{1}H NMR ($CDCl_3$) δ 1.32 (d, J = 6.9 Hz, 3H), 2.24 (t, J = 5.6 Hz, 1H), 3.68 (m, 1H), 3.87 (m, 1H), 4.29 (m, 1H), 6.00 (s, 1H), 7.56 (td, J = 1.5, 5.8 Hz, 1H), 7.60 (dd, J = 1.4, 8.1 Hz, 1H), 7.69 (td, J = 1.2, 7.45 Hz, 1H), 8.09 (dd, J = 1.1, 8.2 Hz1H); ^{13}C NMR ($CDCl_3$) δ 16.6, 48.2, 65.9, 124.5, 128.8, 130.4, 133.0, 133.8, 146.2, 166.7; HRMS (ES) m/z [Na]$^+$ 247.0689 (calcd for $C_{10}H_{12}N_2O_4Na^+$ 247.0689).

***N*-(2-Chloro-(1*S*)-1-methylethyl)-2-nitrobenzamide (4b).** To a solution of **4a** (0.99 g, 4.39 mmol) in $CHCl_3$ (24 mL) was added $SOCl_2$ (1.05 g, 641 μL, 8.79 mmol). The reaction was heated at reflux for 30 min. The reaction was cooled to room temperature and concentrated under vacuum. The resultant residue was purified by column chromatography on silica using 2% EtOAc/CH_2Cl_2, affording the product as a white solid (1.03 g, 4.24 mmol, 97%): mp 113−114 °C (CH_2Cl_2); ^{1}H NMR ($CDCl_3$) δ 1.39 (d, J = 6.7 Hz, 3H), 3.70 (dd, J = 3.4, 11.2 Hz, 1H), 3.88 (dd, J = 4.2, 11.2 Hz, 1H), 4.58 (m, 1H), 6.00 (d, J = 6.3 Hz, 1H) 7.53 (dd, J = 1.4, 7.5 Hz, 1H) 7.60 (td, J = 1.5, 7.8 Hz, 1H), 7.69 (td, J = 1.2, 7.5 Hz, 1H), 8.09 (dd, 1.0, 8.2 Hz, 1H); ^{13}C NMR ($CDCl_3$) δ 17.5, 46.1, 48.9, 124.6, 128.7, 130.6, 132.7, 133.8, 146.3, 166.0; HRMS (ES) m/z [Na]$^+$ 265.0367 (calcd for $C_{10}H_{11}ClN_2O_3Na^+$ 265.0350).

(4*S*)-4-Methyl-2-(2-nitrophenyl)-4,5-dihydro-1,3-oxazole (5a). To a suspension of NaH (0.34 g, 8.50 mmol, 60% dispersion in oil) in THF (11 mL) was slowly added a solution of **4b** (1.03 g, 4.25 mmol) in THF (10 mL). The reaction was stirred at room temperature for 1 h and then filtered to remove salts and concentrated. The resultant residue was purified by column chromatography on silica using 2% EtOAc/CH_2Cl_2, affording the product as a colorless oil (0.80 g, 3.87 mmol, 91%): ^{1}H NMR ($CDCl_3$) δ 1.37 (d, J = 6.6 Hz, 3H), 3.97 (t, J = 7.8 Hz, 1H), 4.39 (m, 1H), 4.51 (dd, J = 8.0, 9.2 Hz, 1H), 7.59 (td, J = 1.8, 7.7 Hz, 1H), 7.63 (td, J = 1.6, 7.5 Hz, 1H), 7.81 (dd, J = 1.8, 7.6 Hz, 1H), 7.84 (dd, J = 1.7, 7.7 Hz, 1H); ^{13}C NMR ($CDCl_3$) δ 20.9, 62.3, 75.0, 123.4, 123.8, 130.9, 131.3, 132.4, 149.1, 160.9; HRMS (ES) m/z [Na]$^+$ 229.0571 (calcd for $C_{10}H_{10}N_2O_3Na^+$ 229.0584).

2-[(4*S*)-4-Methyl-4,5-dihydro-1,3-oxazol-2-yl]aniline (5b). To a solution of **5a** (0.77 g, 3.72 mmol) in EtOAc (18.6 mL) was added Pd/C (0.08 g). The reaction was placed under an

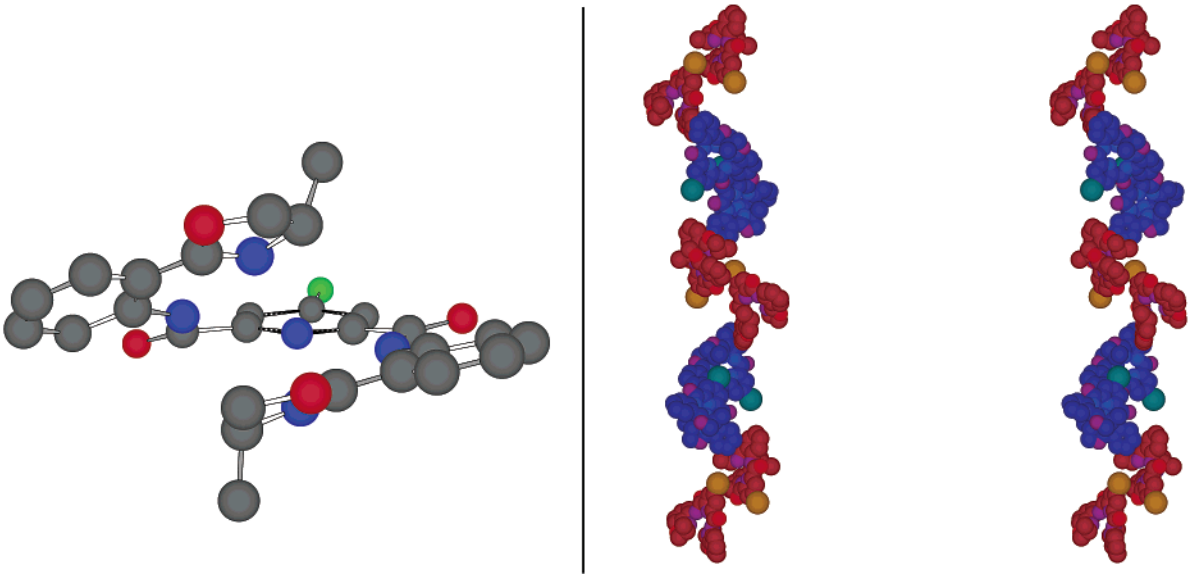

FIGURE 5. X-ray crystal structure of **2a** (left) and stereodepiction of associated crystal lattice (right).

atmosphere of H_2 (balloon) and stirred for 20 h. The reaction was filtered through Celite to remove Pd/C and concentrated. The resultant residue was purified by column chromatography on silica using 5% EtOAc/hexanes, affording the product as a colorless oil (0.58 g, 3.31 mmol, 89%): ^{1}H NMR ($CDCl_3$) δ 1.35 (d, J = 6.5 Hz, 3H), 3.85 (m, 1H), 4.43 (m, 2H,), 6.08 (bs, 2H), 6.66 (ddd, J = 1.1, 7.3, 8.1 Hz, 1H), 6.70 (dd, J = 0.9, 8.2 Hz, 1H), 7.20 (ddd, J = 1.6, 7.2, 8.5 Hz, 1H), 7.69 (dd, J = 1.5, 7.9 Hz, 1H); ^{13}C NMR ($CDCl_3$) δ 21.7, 62.1, 72.2, 109.2, 115.6, 116.0, 129.5, 131.9, 148.5, 163.5; HRMS (ES) m/z $[H]^+$ 177.1028 (calcd for $C_{10}H_{13}N_2O^+$ 177.1022).

4-Chloro-2,6-bis[2-((4*S*)-4-methyl-4,5-dihydro-1,3-oxazol-2-yl)phenyl]carbamoylpyridine (2a). To a stirred solution of **5b** (0.16 g, 0.92 mmol) in CH_2Cl_2 (4 mL) and pyridine (1 mL) with activated 4 Å sieves was added 4-chloropyridine-2,6-dicarbonyl chloride (0.11 g, 0.46 mmol). The reaction was stirred at room temperature for 3 h and then filtered to remove sieves and concentrated. The resultant residue was dissolved in CH_2Cl_2 (50 mL) and washed with saturated $NaHCO_3$ (50 mL). The aqueous layer was back-extracted with CH_2Cl_2 (2 × 25 mL), and the organic phases were combined, dried over $MgSO_4$, filtered, and concentrated, affording product as a white crystalline solid (0.23 g, 0.44 mmol, 96%). The crude product was determined to be of high purity by TLC (10% EtOAc/hexanes) and ^{1}H NMR (further purification can be achieved by column chromatography on silica using 10% EtOAc/hexanes): mp 161−162 °C (CH_2Cl_2); ^{1}H NMR ($CDCl_3$) δ 1.00 (d, J = 6.6 Hz, 6H), 3.70 (t, J = 8.2 Hz, 2H), 3.95 (m, 2H), 4.26 (t, J = 8.7 Hz, 2H), 7.19 (t, J = 7.7 Hz, 2H), 7.57 (td, J = 1.6, 7.9 Hz, 2H), 7.89 (dd, J = 1.5, 7.8 Hz, 2H), 8.40 (s, 2H) 8.92 (d, J = 8.3 Hz, 2H), 13.72 (s, 2H); ^{13}C NMR ($CDCl_3$) δ 20.9, 62.1, 72.7, 115.0, 120.6, 123.3, 125.5, 129.3, 132.4, 138.9, 147.5, 151.9, 162.1, 162.4; HRMS (ES) m/z $[Na]^+$ 540.1404 (calcd for $C_{27}H_{24}ClN_5O_4Na^+$, 540.1410). Anal. Calcd for $C_{27}H_{24}ClN_5O_4$: C, 62.61; H, 4.67; N, 13.52. Found: C, 62.37; H, 4.72; N, 13.33.

4-Thiobenzyl-2,6-bis[2-((4*S*)-4-methyl-4,5-dihydro-1,3-oxazol-2-yl)phenyl]carbamoylpyridine *(2b).* To a suspension of NaH (24 mg, 0.59 mmol, 60% dispersion in oil) in THF (0.5 mL) was added benzyl mercaptan (50.0 mg, 47 μL, 0.40 mmol). The reaction was stirred for 30 min, then a solution of **2a** (52.0 mg, 0.10 mmol) in THF (0.5 mL) was added and the reaction heated to 50 °C for 14 h. The reaction was filtered to remove salts and concentrated. The resultant residue was purified by column chromatography on silica with 10% EtOAc/hexanes, affording the product as a white glassy solid (44.0 mg, 0.073 mmol, 72%): mp 174−175 °C (CH_2Cl_2); ^{1}H NMR ($CDCl_3$) δ 1.00 (d, J = 6.6 Hz, 6H), 3.67 (t, J = 8.2 Hz, 2H), 3.95 (m, 2H), 4.24 (dd, J = 8.1, 1.1 Hz, 2H), 4.38 (s, 2H), 7.17 (td, J = 1.0, 7.6 Hz, 2H), 7.30 (bt, J = 7.3 Hz, 1H), 7.37 (t, J = 7.4 Hz, 2H), 7.48 (d, J = 7.3 Hz, 2H), 7.56 (td, J = 1.5, 7.9 Hz, 2H), 7.89 (dd, J = 1.5, 7.9 Hz, 2H), 8.25 (s, 2H), 8.92 (dd, J = 0.6, 8.3 Hz, 2H), 13.62 (s, 2H); ^{13}C NMR ($CDCl_3$) δ 20.9, 35.8, 62.1, 72.7, 115.0, 120.6, 121.4, 123.1, 127.9, 128.9, 129.2, 132.2, 135.0, 139.0, 150.0, 153.3, 162.0, 163.3; HRMS (ES) m/z $[Na]^+$ 628.1998 (calcd for $C_{34}H_{31}N_5O_4SNa^+$, 628.1989).

***N*-[2-((4*S*)-4-Methyl-4,5-dihydrooxazol-2-yl)phenyl]acetamide (6).** To a solution of **5b** (36 mg, 0.21 mmol), DMAP (3.0 mg, 0.025 mmol), and Et_3N (6.2 mg, 86 μL, 0.62 mmol) in CH_2Cl_2 (1 mL) at 0 °C was added acetic anhydride (42.0 mg, 39 μL, 0.41 mmol). The reaction warmed to room temperature over 27 h and then was concentrated in vacuo. The resultant residue was purified by column chromatography on silica with 10% EtOAc/hexanes, affording the product as a white crystalline solid (17.0 mg, 0.078 mmol, 38%): mp 70−71 °C (CH_2Cl_2); ^{1}H NMR ($CDCl_3$) δ 1.39 (d, J = 6.5 Hz, 3H), 2.22 (s, 3H), 3.92 (m, 1H), 4.48 (m, 2H), 7.07 (td, J = 1.2, 7.6 Hz, 1H), 7.46 (td, J = 1.6, 7.9 Hz, 1H) 7.84 (dd, J = 1.6, 7.9 Hz, 1H), 8.72 (dd, J = 0.85, 8.5 Hz, 1H), 12.24 (s, 1H); ^{13}C NMR ($CDCl_3$) δ 21.6, 25.3, 62.0, 72.0, 113.0, 119.6, 122.1, 129.1, 132.5, 140.0, 163.4, 169.2; HRMS (ES) m/z $[Na]^+$ 241.0941 (calcd for $C_{12}H_{14}N_2O_2Na^+$, 241.0947).

Acknowledgment. This work was supported by the National Science Foundation NSE program (CHE-0103133). Acknowledgment is also made to the donors of the Petroleum Research Fund, administered by the American Chemical Society for partial support of this work.

Supporting Information Available: Tables of X-ray structural data and ORTEP diagrams for **2a**, Gaussian output for the TDDFT calculations of **6**, and ^{1}H NMR spectra for all new compounds. This material is available free of charge via the Internet at http://pubs.acs.org.

JO026496F